

# Adeno Associated Virus 9–Based Gene Therapy Delivers a Functional Monocarboxylate Transporter 8, Improving Thyroid Hormone Availability to the Brain of *Mct8*-Deficient Mice

Hideyuki Iwayama,<sup>1</sup> Xiao-Hui Liao,<sup>1</sup> Lyndsey Braun,<sup>2,3</sup> Soledad Báñez-López,<sup>4,5</sup> Brian Kaspar,<sup>2,3</sup> Roy E. Weiss,<sup>6</sup> Alexandra M. Dumitrescu,<sup>1</sup> Ana Guadaño-Ferraz,<sup>4,5</sup> and Samuel Refetoff<sup>1,7,8</sup>

**Background:** *MCT8* gene mutations produce thyroid hormone (TH) deficiency in the brain, causing severe neuropsychomotor abnormalities not correctable by treatment with TH. This proof-of-concept study examined whether transfer of human *MCT8* (*hMCT8*) cDNA using adeno-associated virus 9 (AAV9) could correct the brain defects of *Mct8* knockout mice (*Mct8KO*).

**Methods:** AAV9 vectors delivering long and/or short *hMCT8* protein isoforms or an empty vector were injected intravenously (IV) and/or intracerebroventricularly (ICV) into postnatal day 1 *Mct8KO* and wild type (*Wt*) mice. Triiodothyronine (T3) was given daily for four days before postnatal day 28, at which time brains were collected after perfusion to assess increase in T3 content and effect on the T3-responsive transcription factor, *Hairless*.

**Results:** Increased pup mortality was observed after IV injection of the *AAV9-long* *hMCT8* isoform, but not after injection of *AAV9-short* *hMCT8* isoform. Compared to IV, ICV delivery produced more *hMCT8* mRNA and protein relative to the viral dose, which was present in various brain regions and localized to the cell membranes. Despite production of abundant *hMCT8* mRNA and protein with ICV delivery, only IV delivered *AAV9-hMCT8* targeted the choroid plexus and significantly increased brain T3 content and expression of *Hairless*.

**Conclusions:** These results indicate that *MCT8* delivery to brain barriers by IV but not ICV injection is crucial for its proper function. *MCT8* has no constitutive activity but acts through an increase in T3 entering the brain tissue. Increasing *MCT8* expression in brain cell membranes, including neurons, is insufficient to produce an effect without an increase in brain T3 content. The correct *hMCT8* isoform along with an optimized delivery method are critical for an effective gene therapy to provide functional *MCT8* in the brain of patients with *MCT8* mutations.

## Introduction

THE *MCT8* (*SLC16A2*) GENE, which encodes a cell membrane protein that serves as a specific transporter of thyroid hormone (TH) (1), is located on the X chromosome. *MCT8* gene mutations in males lead to severe neuropsychomotor deficits (e.g., inability to sit or walk independently and a lack of speech or a severely dysarthric speech), hypermetabolism in peripheral tissues, and an unusual combination of thyroid function test abnormalities (high serum levels of

triiodothyronine [T3], low levels of reverse T3 [TSH] and thyroxine [T4], and a normal or slightly elevated thyrotropin) (2,3). Defective *MCT8* proteins reduce TH transport into the brain, producing tissue TH deprivation and delayed myelination (4–6). This form of sex-linked mental retardation has been named the Allan–Herndon–Dudley syndrome and was initially described by these authors in 1944 (7). Later, such patients were found by Schwartz *et al.* (8) to have *MCT8* gene mutations and TH test abnormalities. Treatment of affected children with a combination of levothyroxine (LT4),

Departments of <sup>1</sup>Medicine and <sup>7</sup>Pediatrics and <sup>8</sup>Committee on Genetics, The University of Chicago, Chicago, Illinois.

<sup>2</sup>Research Institute at Nationwide Children’s Hospital, Columbus, Ohio.

<sup>3</sup>Department of Neuroscience, The Ohio State University, Columbus, Ohio.

<sup>4</sup>Instituto for Biomedical Research “Alberto Sols,” Consejo Superior de Investigaciones Científicas-Universidad Autónoma de Madrid, Madrid, Spain.

<sup>5</sup>Center for Biomedical Research on Rare Diseases (Ciberer), Instituto de Salud Carlos III, Madrid, Spain.

<sup>6</sup>Department of Medicine, University of Miami, Miami, Florida.

propylthiouracil (PTU), or the thyromimetic compound diiodothyropropionic acid (DITPA) reduces the hypermetabolism and ameliorates nutrition, but does not produce significant neurodevelopmental improvements (9,10).

Adeno-associated virus (AAV) is a small non-pathogenic virus that can infect various species (11). Its use in gene therapy has several advantages, encompassing limited immune response, the ability to infect various cell types including post-mitotic cells, and persistence without integration into host chromosomes. AAV9 has been shown to transduce the brain with high efficiency following delivery into the bloodstream or into the cerebrospinal fluid (12). Therefore, it was hypothesized that AAV9 could be a good candidate for viral transfer of MCT8 into the MCT8-deficient brain.

Human MCT8 (hMCT8) has two isoforms with different amino acid lengths of 613 or 539, due to translation from separate ATG start codons. Mouse *Mct8* only generates a 545 amino acid isoform, which is shorter at the intracellular amino terminus (Supplementary Fig. S1; Supplementary Data are available online at [www.liebertpub.com/thy](http://www.liebertpub.com/thy)). In both species, the first of the 12 transmembrane domains starts at a QPPE motif, located at amino acids 167–170 of the long form of the hMCT8. Until recently, the relevance of the two human hMCT8 isoforms was unknown, but it has now been shown that the long form is more rapidly degraded (13). Short hMCT8 and mouse *Mct8* have 95.4% similarity, but their antigenicity is different (14,15).

The current study examined the efficacy of an AAV9 vector to transfer the short (S) and the long (L) *hMCT8* cDNA (AAV9-*ShMCT8* and AAV9-*LhMCT8*, respectively) to the *Mct8KO* mouse at postnatal day 1 (P1) using either intravenous (IV) or intracerebroventricular (ICV) delivery. Pup survival was significantly higher following IV injection of the *ShMCT8* isoform compared with the *LhMCT8* isoform. Even though ICV delivery resulted in higher dose-dependent levels of MCT8 mRNA and protein targeted to nerve cell membranes, only IV-delivered AAV9-*ShMCT8* increased brain T3 content and expression of the TH-induced transcription factor *Hairless* (*Hr*). This indicates that (i) MCT8 lacks constitutive activity, (ii) its expression in nerve cell membranes does not enhance the effect of T3, (iii) its delivery to the brain barriers is critical for mediating T3 action, and (iv) that this occurs only with IV delivery of the vector expressing MCT8. The current report highlights that it is necessary to optimize the gene isoform and delivery strategies in order to provide functional hMCT8 to the brain successfully for the treatment of MCT8 deficiency.

## Materials and Methods

### Virus

AAV9 was produced as previously described (16). The *hMCT8* cDNA expression constructs were cloned into the polylinkers of dsAAV CB MCS. The virus was produced in HEK293 cells by transient transfection followed by purification using gradient density steps, dialyzed against phosphate-buffered saline (PBS) with 0.001% Pluronic-F68 to prevent virus aggregation, and was stored at 4°C. All vector preparations were titrated by quantitative polymerase chain reaction (qPCR) using Taq-Man technology. Two lengths of *hMCT8* cDNA, encoding proteins of 613 amino

acids (*LhMCT8*) and 539 amino acids (*ShMCT8*), were used for the experiments.

### Experimental animals

All procedures carried out in mice were conducted in accordance with the accepted standards of humane animal care as outlined in the Ethical Guidelines and were approved by the Institutional Animal Care and Use Committee.

*Mct8KO* mice, in C57Bl/6J background, were generated and housed as described previously (17). Male *Mct8KO* (*Mct8*<sup>-/-</sup>) and *Wt* (*Mct8*<sup>+/+</sup>) litter mates were produced by mating heterozygous females (*Mct8KO*<sup>+/-</sup>) with *Wt* males. A total of 110 newborn male mice were used in the experiments. AAV9-*hMCT8* or Empty Vector (EV), as control, were injected into mice at P1 IV (low  $8 \times 10^{10}$ , middle  $2 \times 10^{11}$ , and high  $4 \times 10^{11}$  viral particles [vp] per mouse), ICV (low  $5 \times 10^9$  and high  $3 \times 10^{10}$  vp dose), or combined IV + ICV (high dose of both). Death occurring prior to P10 (nine days after virus injection) was scored. Mice were injected daily intraperitoneally (IP) with liothyronine (LT3; 5  $\mu$ g/100 g body weight/day) for four consecutive days. At P28 and six hours after the last injection of LT3, blood was obtained for T3 measurement, after which animals were perfused under anesthesia with heparinized PBS through a needle placed in the left ventricle before tissue harvesting. For histological, immunohistochemical, and immunofluorescent analyses, mice were killed at P28 without LT3 treatment, and paraformaldehyde was used in the perfusate prior to brain collection.

### Extraction and measurement of tissue mRNA

Brain tissues were collected after perfusion, and immediately frozen on dry ice and stored at -80°C. Total RNA was extracted from the cerebrum (cerebral hemispheres without cerebellum), and mRNAs were measured by qPCR as previously described (17). To evaluate the efficacy of viral treatment, the expression of the TH regulated gene *Hr* was quantitated by qPCR (18,19). The housekeeping gene, *RNA polymerase II* (*RpII*), was used as internal control (Supplementary Table S1).

### Measurements of T3 in serum and tissues

T3 in serum and tissues were measured by a specific radioimmunoassay as previously described in detail (see supplement to Ferrara *et al.*) (20).

### Western blotting

Brain tissue was homogenized in 0.1 M of KPO<sub>4</sub> pH 7, 1 mM of EDTA, and 4 mM of DTT in the presence of phenylmethylsulfonyl fluoride as protease inhibitor, and 40  $\mu$ g of protein was loaded in each well of a 8% SDS-PAGE. After electrophoresis and transfer onto a polyvinylidene fluoride membrane, the latter were exposed to Tris-buffered saline with Tween 20 (TBST) buffer with 5% of ECL blocking agent (RPN2125; GE Healthcare). The primary antibody against hMCT8 (HPA003353; Sigma) was diluted 1:1000 in TBST, and the secondary anti-rabbit IgG (#3460; Thermo Scientific) was used in 1:25,000 dilution. Chemiluminescence was developed with ECL blotting reagents (RPN2109; GE Healthcare). Bands were quantitated by Image J v1.34 S and corrected for glyceraldehyde 3-phosphate dehydrogenase (GAPDH).

### Histological processing

Mice were transcardially perfused under anesthesia with 4% paraformaldehyde in 0.1 M PBS. Brains were then removed and postfixed for 24 h and afterwards embedded in paraffin. Paraffin blocks containing cerebral cortex were cut coronally, while those containing cerebellum were cut sagittally into 8  $\mu$ m thick sections that were transferred onto Superfrost Ultra Plus slides (J3800AMNZ; Thermo Scientific).

### Immunohistochemical and immunofluorescence procedures

After deparaffination and rehydration, tissue sections were incubated at 95°C in an oven for 20 min with the EnVision FLEX Low pH (K8005; Dako, Aligent Technologies) solution for antigen retrieval. For diaminobenzidine labeling, endogenous peroxidase activity was blocked with 3% hydrogen peroxide in distilled water at room temperature for 15 min. Nonspecific protein binding was prevented by blocking the tissue in PBS containing 0.1% Triton X-100, 4% bovine serum albumin (BSA), and 5% normal goat serum (S-1000; Vector Laboratories) at room temperature for 1.5 h. Tissue sections were incubated at 4°C overnight with the primary rabbit anti-hMCT8 serum, 1:250 (HPA003353; Sigma) in PBS containing 0.1% Triton X-100, 4% BSA, and 1% normal goat serum. A biotinylated anti-rabbit secondary antibody (BA-1000; Vector Laboratories) was used at a 1:200 dilution in PBS containing 0.1% Triton, 4% BSA, and 1% normal goat serum at room temperature for 1 h. For signal amplification, the sections were incubated with Avidin-Biotin Complex (Ultra-Sensitive ABC Peroxidase Staining Kits, 32050; Thermo Scientific) at room temperature for 1 h and revealed with diaminobenzidine (D5637, 5 mg/mL; Sigma). Some preparations were counterstained with Harris hematoxylin (HHS32; Sigma). Finally, tissues were dehydrated in ascending (50%, 70%, 96%, and 2  $\times$  100%) alcohol concentrations, cleared in xylenes, and covered with the hydrophobic mounting medium Depex (18243; Serva). Furthermore, in order to verify the specificity of the secondary antibody, negative controls were run in parallel without the primary antibody.

For immunofluorescence labeling, after antigen retrieval, nonspecific binding was prevented in the same way as in the diaminobenzidine labeling. Then, the sections were incubated at 4°C overnight with the primary rabbit anti-hMCT8 serum, 1:200 (HPA003353; Sigma) in PBS containing 0.1% Triton X-100, 4% BSA, and 1% normal goat serum. The secondary antibody goat anti-rabbit Alexa 546 (A-11035; Molecular Probes) was used at a 1:500 dilution in PBS containing 0.1% Triton, 4% BSA, and 1% normal goat serum at room temperature for 2 h. The slices were then washed in PBS and incubated with 4',6-diamidino-2-phenylindole (D1306; DAPI, Molecular Probes) 1:500 in PBS. After washing in PBS, slices were mounted with ProLong Gold Antifade Mountant (P36930; Molecular Probes). Omitting the primary antibodies in the incubation reaction gave no signal.

### Microscopy

Immunohistochemical analyses were made under bright field illumination using a Nikon Eclipse 80i microscope ( $\times$ 20, Numerical Aperture 0.50 and  $\times$ 40, Numerical Aperture

0.75). Photomicrographs were acquired using a Nikon DS-Fi1 digital camera. Immunofluorescence analyses were first made under the fluorescence Zeiss Axiophot microscope (Carl Zeiss). Confocal images were acquired using an inverted Zeiss LSM710 Laser Scanning Microscope (Carl Zeiss) with Plan-Apochromat 63  $\times$  oil-immersion objectives (1.40 NA) without or at 2  $\times$  zoom. A sequential scanning mode was used to avoid crosstalk between channels. Negative control tissue sections (without primary antibodies) were used for background setting prior to image acquisition. The images were analyzed and processed (maximum intensity projections of Z-series) using ImageJ software (1.48v; National Institutes of Health).

### Statistical analysis

All results are expressed as mean  $\pm$  standard error of the mean (SEM). Statistical analysis of multiple groups was performed by one-way analysis of variance. Student's *t*-test was used when there were only two groups to compare. *p*-Values of <0.05 were considered to be significant.

## Results

### *hMCT8* isoforms and doses exhibit differential safety

*Mct8KO* mice at P1 received EV as a control or AAV9-*ShMCT8* or AAV9-*LhMCT8* at escalating doses (IV: low  $8 \times 10^{10}$ , middle  $2 \times 10^{11}$ , and high  $4 \times 10^{11}$  vp/mouse; or ICV: low  $5 \times 10^9$  and high  $3 \times 10^{10}$  vp/mouse). In order to assess the safety of viral delivery, mouse pup death was scored daily until P10. As expected, mice injected with EV showed 90% survival (data not shown). It was found that the high dose of AAV9-*ShMCT8* given IV, ICV, and IV + ICV resulted in 85–88% survival (Fig. 1A). AAV9-*LhMCT8* given IV at the low dose resulted in 94% survival. However, when given at the high dose, IV and IV + ICV resulted in only 9% and 0% survival, respectively (Fig. 1B), with 60% of mice

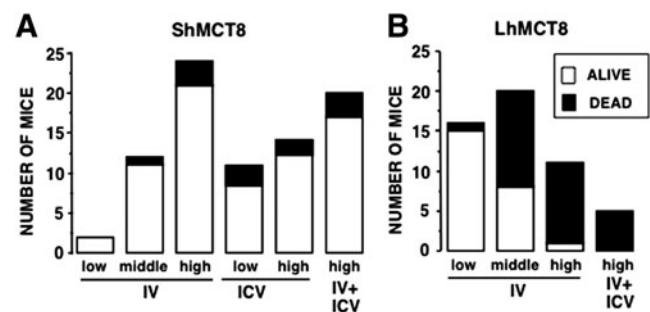


**FIG. 1.** Survival of mice up to nine days after administration of AAV9-*ShMCT8* and AAV9-*LhMCT8* at postnatal day 1 (P1). (A) Between 85% and 92% of the pups given AAV9-*ShMCT8* survived, irrespective of viral dose or route of administration. This was not significantly different from survival after injection of empty vector (EV). (B) Survival of mice injected with AAV9-*LhMCT8* decreased with increased viral dose. Only 9% of the mice injected intravenously (IV) with a high dose were alive at P10. For IV injections, low, middle, and high doses were  $8 \times 10^{10}$ ,  $2 \times 10^{11}$ , and  $4 \times 10^{11}$  viral particles (vp)/mouse, respectively. For mice injected intracerebroventricularly (ICV), low and high doses were  $5 \times 10^9$  and  $3 \times 10^{10}$  vp/mouse, respectively

found dead on P3. Collectively, these data indicate that ShMCT8 is safe while LhMCT8 is toxic in a dose-dependent manner.

#### *Viral delivery of hMCT8 leads to hMCT8 mRNA and protein in the brain*

Given that AAV9-*ShMCT8* administration to the mouse appeared safe, next it was determined whether this hMCT8 isoform could be successfully delivered to the brain using either IV or ICV administration. qPCR with human specific primers, to quantify *hMCT8* in the mouse brain, showed that IV-injected AAV9-*ShMCT8* was transcribed in a dose-dependent manner in the cerebrum (cerebral hemispheres minus cerebellum and brainstem) of *Wt* and *Mct8KO* mice (Fig. 2A). Importantly, ICV injection provided 10–40-fold more mRNA than IV injection, even when given at a dose that was one order of magnitude lower (Fig. 2A left panel vs. the two panels on the right; note difference in scale). The cerebrum of *Mct8KO* mice injected with EV had no detectable *hMCT8* mRNA (data not shown). Western blotting using a hMCT8 antibody was performed to assess whether the transcribed *hMCT8* was translated into protein (Fig. 2B). The expected molecular weight of hMCT8 is 60 kDa, suggesting that the 120 kDa band is a dimer (21). The ShMCT8 isoform showed similar amounts of monomers and dimers (Fig. 2B, lanes 4, 5, and 6). ICV injection of AAV9-*ShMCT8* produced substantially more translated protein for the dose injected (one order of magnitude less) than IV injection of AAV9-*ShMCT8*, which is consistent with the results for *ShMCT8* mRNA in the brain (Fig. 2A). EV-injected mice had no detectable hMCT8 protein (Fig. 2B, lane 2); note the quantification of MCT8 monomer and dimer, normalized with GAPDH used as a loading control, shown in Figure 2C. Collectively, these data show that both RNA and protein were present in the *Mct8KO* mouse brain following IV and ICV delivery, though ICV delivery provided more *hMCT8* mRNA and protein than IV delivery did. The AAV-9 containing the full-length cDNA, *LhMCT8*, was also transcribed and translated in the brain following IV injection (Fig. 2A, right panel, and Fig. 2B, lanes 8 and 9). However, due to its clear toxicity, a decision was made to focus on the ShMCT8 isoform for further evaluation of the protein distribution and function.

#### *hMCT8 protein localizes to several brain regions of AAV9-ShMCT8 treated mice*

It is important not only to confirm hMCT8 protein production but also to determine the location of the protein within the mouse brain. To localize the distribution of the AAV9-delivered hMCT8 protein, brains of perfused mice were harvested, sectioned, and immunolabeled with a hMCT8 antibody that partially reacts with mouse Mct8 (Supplementary Fig. S1 and Fig. 3). Mct8 protein was faintly detected in the cerebral cortex and cerebellum of the *Wt* mice (Fig. 3A and B) and even to a lesser degree in *Mct8KO* mice (Fig. 3D and E) both given EV. However, it was clearly detected in the choroid plexus of the same *Wt* mouse (Fig. 3C), but not in the corresponding region of the *Mct8KO* mouse brain (Fig. 3F). These results can be explained as follows. First, the partial immunoreactivity of the antibody with mouse Mct8 stained regions of the *Wt* mouse brain with

very high expression of the mouse Mct8, such as the choroid plexus. Second, the *Mct8KO* mice generated by deleting exon 3 likely synthesize the amino terminal fraction of the transporter, producing a faint staining in the cerebral cortex and the Purkinje cells of *KO* mice using an antibody against the amino terminus of the molecule.

Following both IV and ICV delivery of AAV9-*ShMCT8* to the *Mct8KO* mouse, the hMCT8 protein was clearly present in the cerebral cortex (Fig. 3G and J), cerebellum (Fig. 3H and K), and choroid plexus (Fig. 3I and L). Compared with IV injection, and in accordance with results from Western blots, ICV injection of *ShMCT8* appeared to produce greater amounts of the hMCT8 protein in cerebral cortex (compare Fig. 3G and J), and this hMCT8 protein appeared as aggregated deposits (Fig. 3J). In general, in both the IV- and the ICV-injected mice, there was higher hMCT8 expression in the cerebral cortex at the granular and infragranular layers of the neocortex and at the CA regions of the hippocampus. Subcortical regions presented few immunopositive cells, and the dentate gyrus presented almost no hMCT8 expression (data not shown). In addition, there was a clear presence of hMCT8 at the dendritic arborizations of some Purkinje cells in the cerebellum of both IV- and ICV-injected mice (Fig. 3H and K and Supplementary Fig. S2). Most remarkable was the robust expression of hMCT8 in the choroid plexus of *Mct8KO* mice following IV-injected AAV9-*ShMCT8*. In contrast to the cortical profile, there appeared to be a larger amount of protein following IV injection compared with ICV injection (Fig. 3I and L). Notably, the distribution of IV-delivered ShMCT8 was identical to the endogenous Mct8 observed in the *Wt* mouse (Fig. 3C and I), whereas ICV-delivered ShMCT8 was minimal and confined to a few cells of the choroid plexus (Fig. 3L). Confocal microscopy demonstrated that hMCT8 was targeted to the apical membrane of epithelial cells of the choroid plexus in IV-injected mice and only to a few cells of mice receiving the virus ICV (Fig. 4A and B). In addition, hMCT8 was targeted to the cell membrane of neurons in both IV- and ICV-injected mice (Fig. 4C–F). An attempt was made to determine whether hMCT8 was delivered to the blood–brain barrier as well as to the choroid plexus. However, the experimental conditions were unable to detect an immune positive signal in endothelial cells of the blood vessels, even after increasing the primary antibody concentration and incubation time.

#### *Viral delivery of hMCT8 leads to increased T3 content in the brain*

As AAV9 clearly delivered hMCT8 protein to the mouse brain, next the functionality of this protein was verified. To do this, 5  $\mu$ g of T3/100 g of body weight IV was administered daily for four days starting at P25 via IP injection. At P28 and six hours after the last injection, the average serum T3 concentration was not significantly different in all mouse groups (Supplementary Fig. S3). Mice were then perfused, and the T3 content in the cerebrum was measured in order to assess TH transport in brain tissue. In *Mct8KO* mice injected IV with AAV9-*ShMCT*, T3 content was 1.5-fold higher with the middle dose and 2.0-fold higher with the high dose above the background of EV-injected *Mct8KO* mice (Fig. 5A). This increase represented 10% and 17%, respectively, of the T3 content in cerebrum of *Wt* mice injected with EV. In contrast,

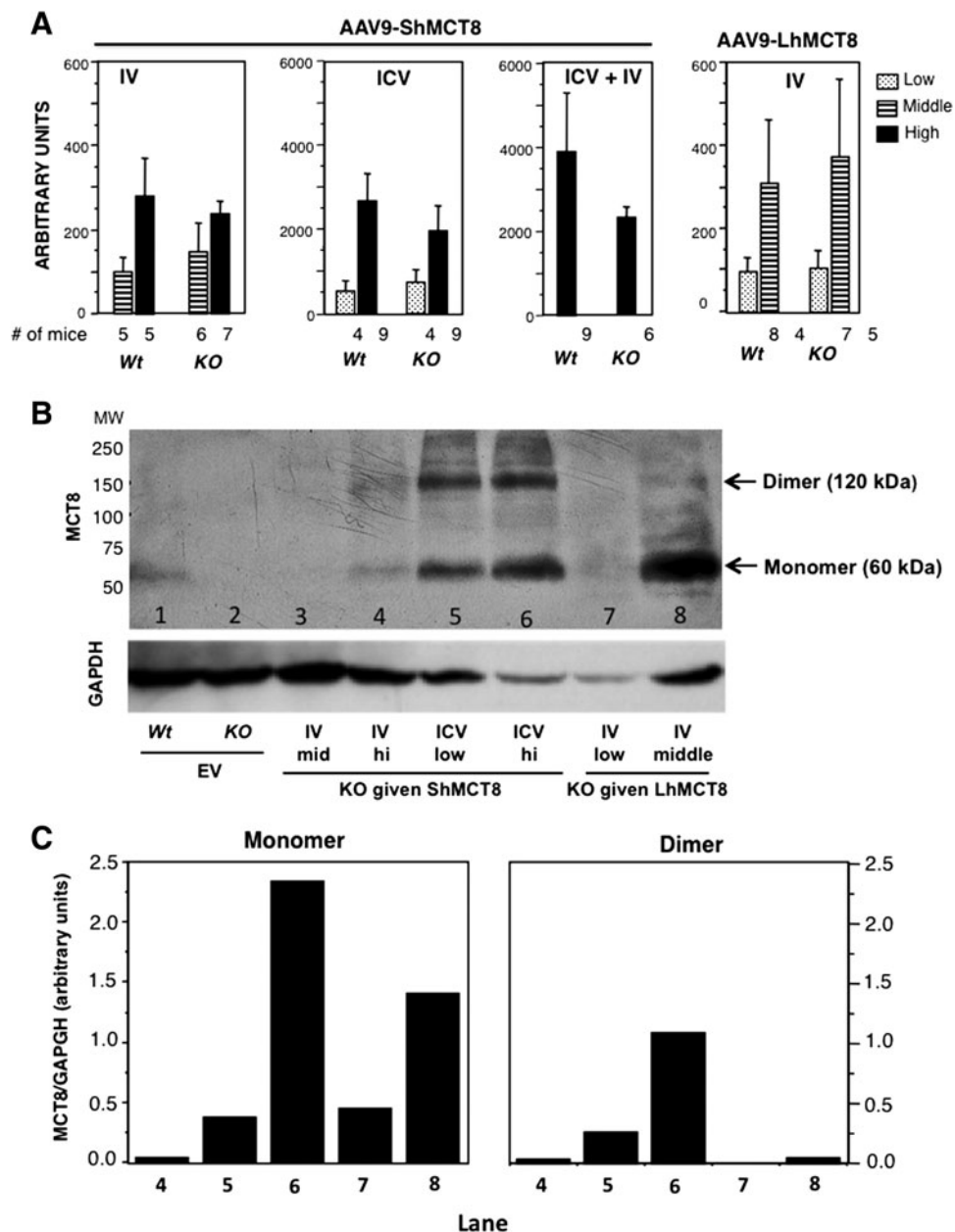


**FIG. 2.** *hMCT8* mRNA and protein in cerebrium of mice injected with AAV9-*ShMCT8* and AAV9-*LhMCT8*. (A) The *MCT8* cDNA contained in the AAV9 transcribed in a dose-dependent manner. Note that the ICV injection induced 10–40 times more mRNA than IV injection did using doses one order of magnitude lower than those used for IV injections. Doses were as follows: for IV administration, low =  $8 \times 10^{10}$ , middle =  $2 \times 10^{11}$ , and high =  $4 \times 10^{11}$  vp per mouse; for ICV administration, low =  $5 \times 10^9$  and high =  $3 \times 10^{10}$  vp/mouse. Results are given as mean  $\pm$  standard error of the mean (SEM). Number (#) of animals per group is indicated. (B) Western blot analysis after SDS-PAGE of cerebrium homogenates developed with an antibody against *hMCT8*. Glyceraldehyde 3-phosphate dehydrogenase (GAPDH) is used as a loading control. In agreement with the mRNA data, vectors injected ICV induced more protein than those injected IV did (lanes 5 and 6 compared with lanes 3 and 4). The expected molecular weight of *hMCT8* is 60 kDa. *ShMCT8* produced a monomer as well as a dimer (lanes 3, 5, and 6). In contrast, *LhMCH8* produced predominantly a monomer (lanes 7 and 8). (C) Quantitative analysis of the *MCT8* in the bands shown in (B), corrected for the GAPDH loading control. Note that the amount of *MCT8* in the brain of the *Wt* mouse given EV was not calculated because of the unknown level of cross-reactivity.

ICV injections of AAV9-*ShMCT8* at both doses did not increase the cerebrium T3 content above background, and ICV injections combined with IV injections (IV + ICV) did not augment the T3 level compared to that achieved with IV injection alone. These data collectively indicate that

AAV9-*ShMCT8* given IV, but not given ICV, can increase T3 content in cerebral tissue.

These results suggest that delivery of *MCT8* to the brain barriers, which does not occur with ICV injection, is crucial for *MCT8* to increase brain T3.

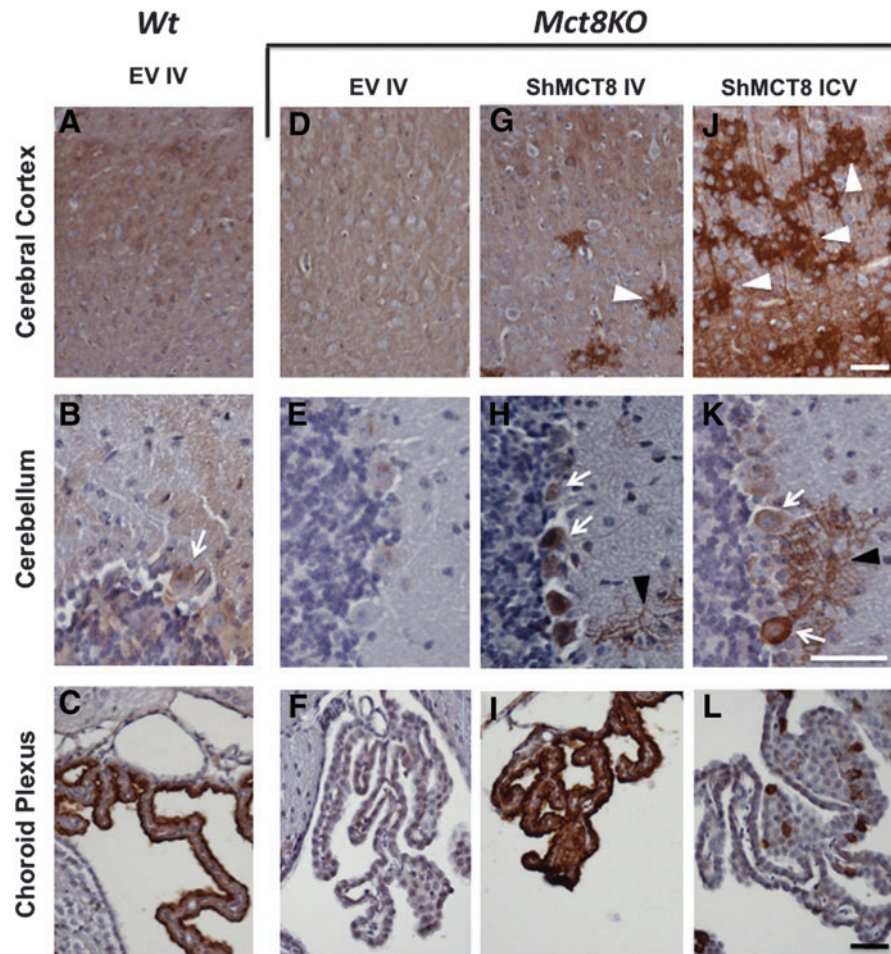


**FIG. 3.** Localization of the expressed hMCT8 protein in brains of *Mct8KO* mice given high doses of AAV9-*ShMCT8* IV ( $4 \times 10^{11}$  vp/mouse) and ICV ( $3 \times 10^{10}$  vp/mouse) compared with *Wt* and *KO* animals injected IV with EV. Representative images showing hMCT8 expression (in brown) detected with a specific antibody by immunohistochemistry counterstained with hematoxylin in the somatosensory region of the cerebral cortex (A, D, G, J), the cerebellar lobule 4 (B, E, H, K), and choroid plexus (C, F, I, L) of *Wt* (A–C) and *Mct8KO* (D–F) mice injected with EV. *Mct8KO* mice were injected with AAV9-*ShMCT8* IV (G–I) or ICV (J–L). In accordance with results from Western blots, hMCT8 was present in larger quantities in the cerebral cortex of mice injected with the virus ICV (J) than IV (G). However, much of the immunoreactivity was present in aggregates (white arrowheads). Some Purkinje cells (white arrows) were observed in both IV- and ICV-injected cerebellum (H and K) with remarkable hMCT8 expression at the dendritic arborizations (black arrowheads). The control, *Wt* mice injected with EV, did not show the positive signal of dendritic arborizations (B). hMCT8 was abundantly present at the choroid plexus of IV-injected *KO* mice (I) and only spottily expressed in mice given the virus ICV (L). The scale bar for each brain region is in the lower right corner of the left photograph and equals  $50 \mu\text{m}$ . Color images available online at [www.liebertpub.com/thy](http://www.liebertpub.com/thy)

#### *Viral delivery of hMCT8 leads to increased expression of Hr in the brain*

Given the significantly increased T3 levels following IV injection of AAV9-*hMCT8*, the functional effect of AAV9-*hMCT8* delivered to the brain of *Mct8KO* mice was further assessed. qPCR was used to measure the expression of the TH-responsive gene *Hr* in the cerebrum. Compared with the control mice (*Mct8KO* injected with EV), *Hr* gene expression doubled when the AAV9-*ShMCT8* was administered IV but not ICV (Fig. 5B). In stark contrast, ICV injections of AAV9-*ShMCT8* at both doses did not increase *Hr* gene expression in the cerebrum above background, and ICV injections combined with IV injections (IV + ICV) did not augment the *Hr* gene expression compared to IV injection alone.

The level of *Hr* gene expression in treated *Mct8KO* mice did not reach that of the *Wt* controls but was nonetheless significantly greater than *Mct8KO* mice receiving EV and was congruent with the increase in T3 content. Once again, only IV delivery of AAV9-*hMCT8* significantly increased brain *Hr* gene expression, suggesting that MCT8 delivery to the brain barriers, which does not occur with ICV injection, is crucial for MCT8 to function and affect *Hr* gene transcription in the brain.

#### Discussion

This work demonstrates that AAV9-*ShMCT8* administered IV but not ICV to the *Mct8KO* mouse causes an increase in brain T3 content and induced subsequent changes in the TH-responsive transcription factor, *Hr*. This occurred despite



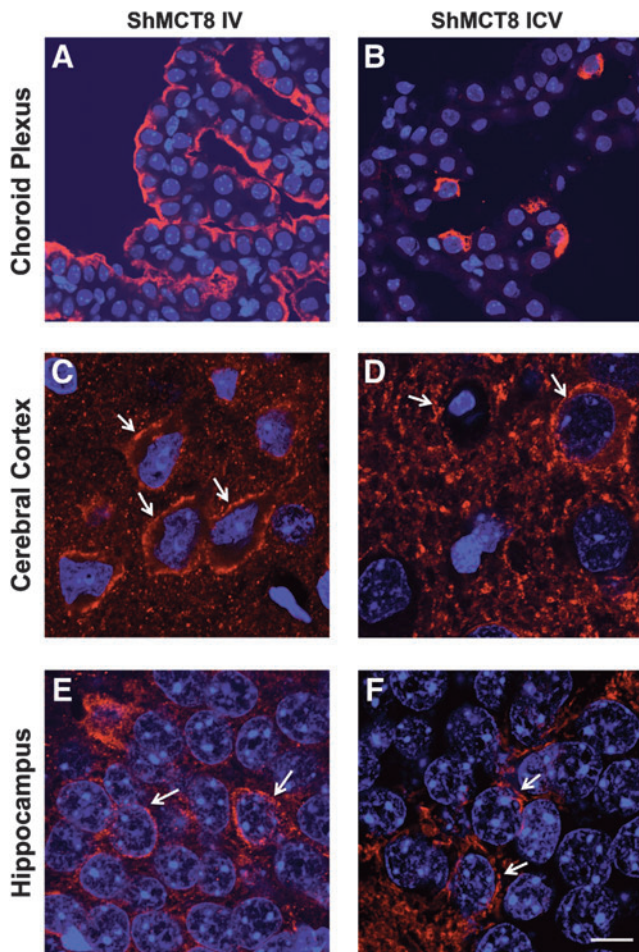


**FIG. 4.** Membrane localization of hMCT8 demonstrated by confocal microscopy in *Mct8KO* mice injected with AAV9-*ShMCT8* IV and ICV (for dose, see legend to Fig. 3). Representative images showing immunopositive signal for hMCT8 (in red) and nuclei stained with DAPI (in blue) in the choroid plexus (A, B), cerebral cortex (C, D) and CA1 region of the hippocampus (E, F) of *Mct8KO* mice injected with AAV9-*ShMCT8* IV (A, C, E) or ICV (B, D, F). hMCT8 was neatly localized at the apical membrane of the choroid plexus of IV-injected mice (A). A similar localization was observed in only few cells of ICV injected animals (B). hMCT8 was localized in the membranes (see white arrows) of cortical and hippocampal neurons of animals injected either IV or ICV (C–F). However, a greater amount of hMCT8 was present in the cytoplasm of animals injected ICV. (A, B) Scale bar = 20  $\mu\text{m}$ ; (C–F) scale bar = 10  $\mu\text{m}$ . Color images available online at [www.liebertpub.com/thy](http://www.liebertpub.com/thy)

substantially more transcription and translation of the same virus administered ICV. Thus, it is concluded that IV injection of AAV9-*ShMCT8* is required for proper targeting of MCT8 to facilitate the delivery of T3 across the brain barriers. This conclusion is supported by immunohistochemistry that shows drastic differences in the localization of MCT8 in the choroid plexus achieved by IV compared with ICV injection.

Normal or mutant *hMCT8* containing plasmids have been transfected into human and other mammalian cells in culture (21). To the authors' knowledge, this is the first report of successful delivery of MCT8 *in vivo* through a viral vector. AAV9 has been used for the treatment of genetic diseases,

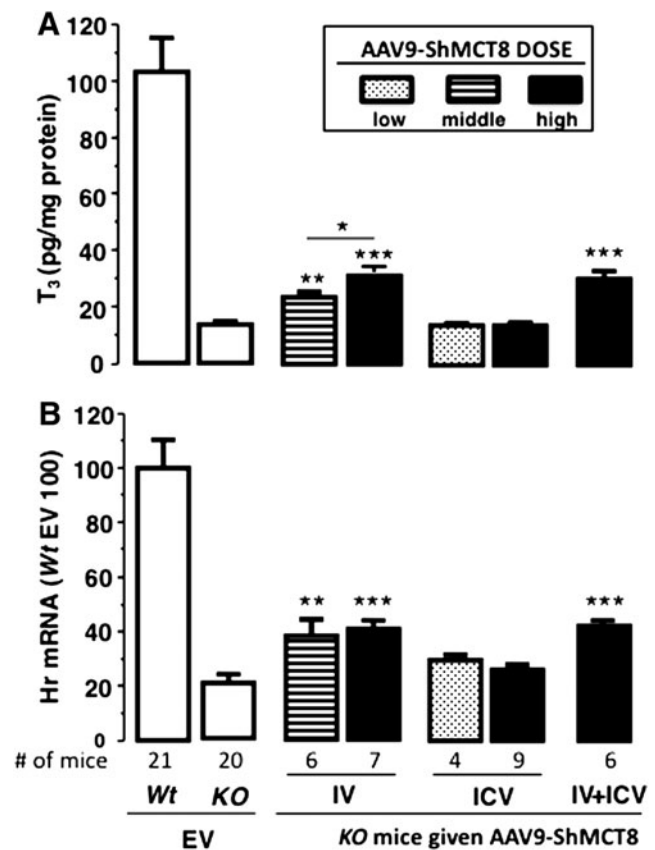


**FIG. 5.** Effect of AAV9-*ShMCT8* on triiodothyronine (T3) content and induction of *Hairless* (*Hr*) expression in the cerebrum of mice injected with the virus IV, ICV, and combined IV + ICV. (A) Cerebrum T3 content. (B) *Hr* gene expression. Relative to *Mct8KO* mice injected with EV, a significant increase in brain T3 content (A) and *Hr* gene expression (B) was observed only in mice injected with the virus IV. Middle and high doses of AAV9-*ShMCT8* injected IV were  $2 \times 10^{11}$  and  $4 \times 10^{11}$  vp/mouse, respectively. For ICV injections, low and high dose were  $5 \times 10^9$  and  $3 \times 10^{10}$  vp/mouse, respectively. The combined IV + ICV injections contained the high doses of virus. Data from EV given IV and ICV were combined in the *Wt* and *Mct8KO* mice, as the EV did not produce any effect compared with non-injected animals of both genotypes. Data are presented as mean  $\pm$  SEM with the number (#) of animals per group as indicated. Results from *Wt* animals given EV are adjusted to 100% in *Hr* expression. Statistical differences for *Mct8KO* animals given *ShMCT8* and compared to the same genotype given EV are indicated above the bars. \* $p < 0.05$ ; \*\* $p < 0.01$ ; \*\*\* $p < 0.001$ .

including cystic fibrosis and Hemophilia B (22). Further, IV and ICV administration of AAV9 has been effective in the gene therapy of spinal muscular atrophy, a lethal congenital neurodegenerative disorder (23,24). This suggested that the AAV9 virus could potentially induce MCT8 transcription and translation into a functional protein that could transport TH *in vivo*.

Based on the gene sequence, humans but not mice have two putative hMCT8 isoforms differing by presence or lack of 74 aminoterminal amino acids. The present results show that mouse pups injected with virus capable of expressing the long human MCT8 isoform had high mortality, reaching 90% in those receiving the higher dose. Recently, it has been shown that short and long isoforms are synthesized

when the full human *MCT8* cDNA, containing the *LhMCT8*, is transfected into polarized and non-polarized cell lines (13). However, the long isoform is subject to ubiquitination and rapid proteasomal degradation. Whether the long form is properly targeted to the membrane and whether it is functional in terms of TH transport is unknown. Although both hMCT8 isoforms are synthesized from the *LhMCT8* cDNA, here it is shown that the cerebrum of animals given AAV9-*LhMCT8* expresses a form that is apparently not dimerizing, unlike the dimers seen with the form synthesized from AAV9-*ShMCT8*. Visser *et al.* (21) reported that the homodimer is more stable than the monomer. Taken together, these observations suggest that death was possibly caused by accumulation of protein that cannot be processed to form dimers and be targeted to the membrane, or saturation of the capacity for ubiquitination and proteasomal degradation of the long isoform causes its aggregation inside the cell. Given the species differences for MCT8 isoforms between mouse and human, future gene therapy studies may need to assess isoform differences by potentially using *in vitro* models with human cell lines or *in vivo* models with non-human primate models. Other causes for increased mortality have been considered such as an immune response, given the molecular differences between human and mouse MCT8. However, forming immune complexes within the brain parenchyma is unlikely given the early death three to nine days after viral injection. Finally, the possibility of a toxic substance in the vehicle is also unlikely, as the same solutions were used for the EV and *ShMCT8* as for the *LhMCT8*.

A significant and critical difference was discovered in the functional effect of hMCT8 when the same AAV9-hMCT8 vector was delivered by ICV compared with IV injection. While a higher level of transcription and translation of hMCT8 occurred by the ICV route, only the hMCT8 provided by the IV route produced a functional effect in terms of increased cerebrum T3 content and expression of the TH-dependent gene, *Hr*. The fact that MCT8 protein synthesis in the brain of ICV-injected animals failed to produce a biological effect differs from previous reports using spinal cord fluid-based delivery. Namely, AAV9, carrying the human *SMN* cDNA, injected directly in the spinal fluid of mice, as well as nonhuman primates, was more effective in producing a widespread transgene expression in spinal cord motor neurons than when given IV (24).

This discrepant result may be explained by the different localization pattern of ICV- and IV-delivered AAV9-*ShMCT8*. Immunohistochemistry showed that both IV and ICV injections of AAV9-*ShMCT8* produced hMCT8 present in the membrane of neural cells and within neuronal processes such as dendrites in the cerebral cortex, hippocampus, and cerebellum. Importantly, however, normal distribution of MCT8 in cells of the choroid plexus was achieved only by IV administration of the AAV9-*ShMCT8*. The choroid plexus and endothelial cells lining blood vessels are the port of entry of T3 from blood and cerebrospinal fluid into the brain. Based on observations in the rat (25), the choroid plexus contributes 20% of the brain TH, which is in agreement with the magnitude of increase in brain T3 content in the current study. Furthermore, it has been shown that provision of T3 into neurons requires the presence of MCT8 in their cell membrane. This cellular membrane necessity may further explain the lack of functional effect from ICV-delivered AAV9-*ShMCT8*, as more

of the MCT8 was observed as aggregated deposits in the ICV-injected mouse. Therefore, it is a logical conclusion that for gene therapy-delivered MCT8 to provide maximal function, the MCT8 must be targeted to the brain barriers, as required for T3 entry into brain tissue, and additionally must reach the cell membrane for TH transport into neural cells.

Surprisingly, no additional biological effect, as measured by expression of *Hr*, was observed in mice receiving the viral vector by combined IV and ICV injections. The precise reason for this observation is unclear. Either the MCT8 has not been properly targeted to cells or the neural cells expressing the transgene are not involved in the TH-mediated response measured in this study. Furthermore, failure of full integration of hMCT8 into the blood-brain barrier could explain the partial rescue of T3 uptake in brains of IV-injected *Mct8KO* mice compared with *Wt* controls. As surface translocation of MCT8 and the consequent uptake of T3 are cell-type specific (26), the failure of doubling the dose of IV-administered AAV9-*ShMCT8* to increase T3 content and *Hr* gene expression substantially may be due to selective delivery of the hMCT8. The latter could be also species specific.

In conclusion, IV-delivered AAV9-*ShMCT8* increased brain T3 content and produced concomitant changes in the TH-controlled gene, *Hr*, within *Mct8KO* mice. This study shows that simply delivering MCT8 to nerve cells without an increase in brain T3 is insufficient to improve the biochemical consequences of MCT8 deficiency in the brain. Thus, MCT8 does not seem to have a constitutive effect. This proof of concept study highlights the necessity of optimizing gene isoform and delivery strategies in order to achieve functional MCT8 within the brain. These are required to target properly MCT8 to the blood brain barriers using AAV9. The mode of delivery is critical to consider in the development of a successful gene therapy for patients with MCT8 deficiency.

### Acknowledgments

The authors would like to thank Dr. Shana Svendsen for critical review and editing of the manuscript. This work was supported by Grants R37DK15070 from the National Institutes of Health to Samuel Refetoff, the National Center for Advancing Translational Sciences of the National Institutes of Health under Award Number KL2TR000431 to Alexandra M. Dumitrescu, the Seymour J. Abrams and Esformes funds for thyroid research, the Sherman family and Grant SAF2014-54919-R from the Plan Nacional de I+D+I, Spain. Soledad Báñez-López is recipient of a predoctoral contract from the FPI program of the Plan Nacional de I+D+I, Spain. The content is solely the responsibility of the authors and does not necessarily represent the official views of the National Institute of Diabetes and Digestive and Kidney Diseases or the National Institutes of Health.

### Author Disclosure Statement

The authors have nothing to disclose.

### References

1. Friesema EC, Ganguly S, Abdalla A, Manning Fox JE, Halestrap AP, Visser TJ 2003 Identification of monocarboxylate transporter 8 as a specific thyroid hormone transporter. *J Biol Chem* **278**:40128–40135.



2. Dumitrescu AM, Liao XH, Best TB, Brockmann K, Refetoff S 2004 A novel syndrome combining thyroid and neurological abnormalities is associated with mutations in a monocarboxylate transporter gene. *Am J Hum Genet* **74**:168–175.
3. Friesema EC, Grueters A, Biebermann H, Krude H, von Moers A, Reeser M, Barrett TG, Mancilla EE, Svensson J, Kester MH, Kuiper GG, Balkassmi S, Uitterlinden AG, Koehle J, Rodien P, Halestrap AP, Visser TJ 2004 Association between mutations in a thyroid hormone transporter and severe X-linked psychomotor retardation. *Lancet* **364**:1435–1437.
4. Gika AD, Siddiqui A, Hulse AJ, Edwards S, Fallon P, McEntagart ME, Jan W, Josifova D, Lerman-Sagie T, Drummond J, Thompson E, Refetoff S, Bönnemann CG, Jungbluth H 2010 White matter abnormalities and dystonic motor disorder associated with mutations in the SLC16A2 gene. *Dev Med Child Neurol* **52**:475–482.
5. La Piana R, Vanasse M, Brais B, Bernard G 2015 Myelination delay and Allan–Herndon–Dudley syndrome caused by a novel mutation in the SLC16A2 gene. *J Child Neurol* **30**:1371–1374.
6. López-Espíndola D, Morales-Bastos C, Grijota-Martínez C, Liao XH, Lev D, Sugo E, Verge CF, Refetoff S, Bernal J, Guadaño-Ferraz A 2014 Mutations of the thyroid hormone transporter MCT8 cause prenatal brain damage and persistent hypomyelination. *J Clin Endocrinol Metab* **99**:E2799–2804.
7. Allan W, Herndon CN, Dudley FC 1944 Some examples of the inheritance of mental deficiency: apparently sex-linked idiocy and microcephaly. *Am J Ment Defic* **48**:325–334.
8. Schwartz CE, May MM, Carpenter NJ, Rogers RC, Martin J, Bialer MG, Ward J, Sanabria J, Marsa S, Lewis JA, Echeverri R, Lubs HA, Voeller K, Simensen RJ, Stevenson RE 2005 Allan–Herndon–Dudley syndrome and the monocarboxylate transporter 8 (MCT8) gene. *Am J Hum Genet* **77**:41–53.
9. Wemeau JL, Pigeyre M, Proust-Lemoine E, d’Herbomez M, Gottrand F, Jansen J, Visser TJ, Ladsous M 2008 Beneficial effects of propylthiouracil plus L-thyroxine treatment in a patient with a mutation in MCT8. *J Clin Endocrinol Metab* **93**:2084–2088.
10. Verge CF, Konrad D, Cohen M, Di Cosmo C, Dumitrescu AM, Marcinkowski T, Hameed S, Hamilton J, Weiss RE, Refetoff S 2012 Diiodothyropropionic acid (DITPA) in the treatment of MCT8 deficiency. *J Clin Endocrinol Metab* **97**:4515–4523.
11. Schultz BR, Chamberlain JS 2008 Recombinant adeno-associated virus transduction and integration. *Mol Ther* **16**:1189–1199.
12. Grimm D, Lee JS, Wang L, Desai T, Akache B, Storm TA, Kay MA 2008 *In vitro* and *in vivo* gene therapy vector evolution via multispecies interbreeding and retargeting of adeno-associated viruses. *J Virol* **82**:5887–5911.
13. Zwanziger D, Fischer J, Biebermann H, Braun D, Schweizer U, Moeller LC, Schmidt M, Führer D 2015 The N-terminus of human monocarboxylate transporter 8 is a target of ubiquitin depending proteosomal degradation (abstract). *Exp Clin Endocrinol Diabetes* **123**:P03–18.
14. Bonen A, Heynen M, Hatta H 2006 Distribution of monocarboxylate transporters MCT1–MCT8 in rat tissues and human skeletal muscle. *Appl Physiol Nutr Metab* **31**:31–39.
15. Di Cosmo C, Liao XH, Dumitrescu AM, Philp NJ, Weiss RE, Refetoff S 2010 Mice deficient in MCT8 reveal a mechanism regulating thyroid hormone secretion. *J Clin Invest* **120**:3377–3388.
16. Foust KD, Salazar DL, Likhite S, Ferraiuolo L, Ditsworth D, Ilieva H, Meyer K, Schmelzer L, Braun L, Cleveland DW, Kaspar BK 2013 Therapeutic AAV9-mediated suppression of mutant SOD1 slows disease progression and extends survival in models of inherited ALS. *Mol Ther* **21**:2148–2159.
17. Dumitrescu AM, Liao XH, Weiss RE, Millen K, Refetoff S 2006 Tissue-specific thyroid hormone deprivation and excess in monocarboxylate transporter (mct) 8-deficient mice. *Endocrinology* **147**:4036–4043.
18. Morte B, Ceballos A, Diez D, Grijota-Martinez C, Dumitrescu AM, Di Cosmo C, Galton VA, Refetoff S, Bernal J 2010 Thyroid hormone-regulated mouse cerebral cortex genes are differentially dependent on the source of the hormone: a study in monocarboxylate transporter-8- and deiodinase-2-deficient mice. *Endocrinology* **151**:2381–2387.
19. Liao XH, Di Cosmo C, Dumitrescu AM, Hernandez A, Van Sande J, St Germain DL, Weiss RE, Galton VA, Refetoff S 2011 Distinct roles of deiodinases on the phenotype of Mct8 defect: a comparison of eight different mouse genotypes. *Endocrinology* **152**:1180–1191.
20. Ferrara AM, Liao XH, Gil-Ibanez P, Marcinkowski T, Bernal J, Weiss RE, Dumitrescu AM, Refetoff S 2013 Changes in thyroid status during perinatal development of MCT8-deficient male mice. *Endocrinology* **154**:2533–2541.
21. Visser WE, Philp NJ, van Dijk TB, Klootwijk W, Friesema EC, Jansen J, Beesley PW, Ianculescu AG, Visser TJ 2009 Evidence for a homodimeric structure of human monocarboxylate transporter 8. *Endocrinology* **150**:5163–5170.
22. Kotterman MA, Schaffer DV 2014 Engineering adeno-associated viruses for clinical gene therapy. *Nat Rev Genet* **15**:445–451.
23. Foust KD, Nurre E, Montgomery CL, Hernandez A, Chan CM, Kaspar BK 2009 Intravascular AAV9 preferentially targets neonatal neurons and adult astrocytes. *Nat Biotechnol* **27**:59–65.
24. Meyer K, Ferraiuolo L, Schmelzer L, Braun L, McGovern V, Likhite S, Michels O, Govoni A, Fitzgerald J, Morales P, Foust KD, Mendell JR, Burghes AH, Kaspar BK 2015 Improving single injection CSF delivery of AAV9-mediated gene therapy for SMA: a dose–response study in mice and nonhuman primates. *Mol Ther* **23**:477–487.
25. Chanoine JP, Alex S, Fang SL, Stone S, Leonard JL, Korhle J, Braverman LE 1992 Role of transthyretin in the transport of thyroxine from the blood to the choroid plexus, the cerebrospinal fluid, and the brain. *Endocrinology* **130**:933–938.
26. Kinne A, Roth S, Biebermann H, Kohrle J, Grueters A, Schweizer U 2009 Surface translocation and tri-iodothyronine uptake of mutant MCT8 proteins are cell type-dependent. *J Mol Endocrinol* **43**:263–271.

Address correspondence to:  
 Samuel Refetoff, MD, CM  
 The University of Chicago MC3090  
 5841 South Maryland Avenue  
 Chicago, IL 60637

E-mail: srefetof@uchicago.edu